Archives of Materials Science and Engineering
Volume 84
Issue 1
March 2017
Pages 34-41
International Scientific Journal published monthly by the World Academy of Materials and Manufacturing Engineering

Mode I and mode II fatigue crack growth resistance characteristics of high tempered 65G steel

T.M. Lenkovskiy [a], V.V. Kulyk [b,*], Z.A. Duriagina [b,c], R.A. Kovalchuk [d], V.H. Topilnytskyy [b], V.V. Vira [a,b], T.L. Tepla [b]
[a] Karpenko Physico-Mechanical Institute of the NAS of Ukraine, ul. Naukova 5, Lviv 79060, Ukraine
[b] Lviv Polytechnic National University, ul. Bandera 12, Lviv, 79013, Ukraine
[c] Katolicki Uniwersytet Lubelski Jana Pawła II, Al. Racławickie 14, 20-950 Lublin, Poland
[d] Hetman Petro Sahaidachnyi National Army Academy, ul. Heroes of Maidan 32, Lviv 79012, Ukraine
* Corresponding e-mail address: kulykvolodymyrvolodymyrovych@gmail.com

ABSTRACT

Purpose: To investigate the fatigue crack growth at normal tension and transverse shear of 65G steel with the high tempered martensite microstructure and to build an appropriate fatigue crack growth rate curves. To determine the main and auxiliary fatigue crack growth resistance characteristics, which are necessary for machine parts life-time estimation at rolling contact fatigue conditions.

Design/methodology/approach: For determination of fatigue crack growth resistance at normal tension a standard compact specimens with edge crack were tested using a hydraulic testing machine and fatigue testing at transverse shear were performed on the I-beam specimens with the edge longitudinal crack using the original testing setup. For crack growth measurement an optical cathetometer B-630 was used. The crack growth rate V was calculated as crack length increment during loading cycles. The stress intensity factor range ΔK was determined by dependence $\Delta K = (1 - R)K_{max}$ accordingly to the standard test methods. To establish crack faces friction factor at transverse shear fragments of fractured beam specimen containing crack faces were cut out and tested as a friction pair according to Amontons Coulomb's law. On the base of test results the fatigue crack growth rate curves in logarithmic coordinates ΔK vs. V were built. These graphical dependencies for normal tension and transverse shear were used for determination of fatigue crack growth resistance characteristics: fatigue threshold ΔK_{th}, fracture toughness ΔK_{fc}, ΔK_{1-2} and ΔK_{2-3} which indicates the beginning and the end of middle-amplitude region of curve, ΔK^*, parameters C and n of Paris's equation. Metallographic and fractographic analyses were performed on the scanning electronic microscope Zeiss EVO 40XVP.

Findings: Empirical dependences of the stress intensity factor range on fatigue crack growth rate at normal tension and transverse shear of 65G steel with the high tempered martensite microstructure are obtained. Based on these graphical dependencies the fatigue thresholds and fracture toughness as well as the parameters of Paris's equation are determined.

Research limitations/implications: The fatigue crack growth on 65G steel under low-, medium- and high-amplitude cyclic loading at normal tension and transverse shear was investigated. The fatigue crack growth rate values for a wide range of stress intensity factor are estimated. On the base of fractographical analysis the features of fracture of high tempered martensite in 65G steel at transverse shear are studied. It is shown that the transverse shear crack faces friction factor for high tempered martensite structure is less than for low tempered martensite.

Practical implications: Using the fatigue crack growth resistance characteristics of 65G steel at normal tension and transverse shear and related fatigue crack growth rate curves it is possible to predict the life-time of machine parts made of steels with high tempered martensite structure, working at rolling contact fatigue conditions.

Originality/value: Complete fatigue crack growth rate curves of 65G steel with tempered martensite structure at normal tension and transverse shear are built and the fatigue crack growth resistance characteristics for both modes of fracture are determined for the first time.

Keywords: 65G steel; High tempered martensite; Crack growth resistance; Fatigue crack growth rate; Normal tension; Transverse shear

Reference to this paper should be given in the following way:

T.M. Lenkovskiy, V.V. Kulyk, Z.A. Duriagina, R.A. Kovalchuk, V.H. Topilnytskyy, V.V. Vira, T.L. Tepla, Mode I and mode II fatigue crack growth resistance characteristics of high tempered 65G steel, Archives of Materials Science and Engineering 84/1 (2017) 34-41.

PROPERTIES

1. Introduction

Nowadays various experimental techniques and research results of high-strength structure materials which are being used in rolling pairs elements working at rolling contact fatigue conditions are quite well represented in literature [1-11]. However, there are some theoretical approaches [12-24] for the stress-strain state and contact strength evaluation of rolling bearings, rolling mills rolls, gears, railway wheels and rails, based on the criteria of contact-fatigue defects formation, such as pittings and shellings (Fig. 1).

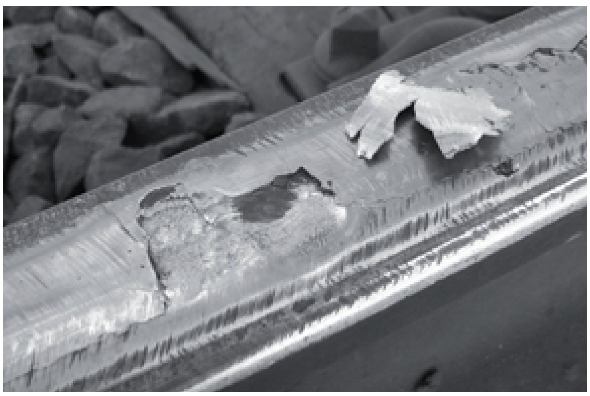

Fig. 1. Shelling on the rail head surface, caused by subsurface fatigue crack spreading

These models take into account the possibility of changing the fracture mode from transverse shear (Mode II) to normal tension (Mode I) and vice versa, kinetics of crack faces contact and friction between them, nonlinearity of crack trajectory and so on.

The numerical calculations on the base of these theoretical approaches requires an appropriate fatigue crack growth rate curves of structural steels, obtained experimentally by testing specimens at normal tension and transverse shear conditions. Due to the lack of effective experimental techniques for transverse shear fatigue testing, such curves and obtained from them fatigue crack growth resistance characteristics are rare in literature [25-31]. So, the work dedicated to fatigue crack growth rate curves building and fatigue crack growth resistance characteristics determination of commonly used structural 65G steel at normal tension and transverse shear is definitely relevant, and the obtained results will find their application in scientific and engineering practice.

2. Experimental procedures

The investigated material for fatigue testing was widely used structural steel of chemical composition given in Table 1 (65G mark according to GOST standards, 65Mn mark according to EN 10027-1:2016). In order to obtain

Table 1.
Chemical composition of investigated steel

Chemical element	C	Si	Mn	Ni	Cr	Cu	S	P
Wt %	0.62-0.7	0.17-0.37	0.9-1.2	< 0.25	≤ 0.25	≤ 0.2	≤ 0.035	≤ 0.035

homogeneous structure specimens were subjected to following heat treatment: quenching from 820°C in oil and subsequent tempering at 650°C for 1 hour.

For determination of fatigue crack growth resistance at normal tension a standard compact specimens of basic dimension b = 45 mm and thickness t = 10 mm with edge crack were tested using a hydraulic testing machine Heckert EUS-20 at stress ratio R = 0.1 and frequency 15 Hz according to recommendations [33]. Fatigue testing at transverse shear were performed on a beam specimens of basic dimension b = 72 mm and wall thickness t = 3.2 mm with the edge longitudinal crack using an original testing setup [34] at stress ratio R = -1 and frequency 12 Hz according to standard [35]. For crack growth measurement an optical cathetometer B-630 equipped with digital camera ToupTech UCMOS 10000KPA was used. The crack growth rate was calculated as $V = \Delta a/\Delta N$, where Δa is a crack length increment during ΔN loading cycles. The stress intensity factor range ΔK was determined by dependence $\Delta K = (1 - R)K_{max}$. So, respectively, at normal tension $\Delta K_I = 0.9K_{I\,max}$, and in the case of transverse shear $\Delta K_{II} = 2K_{II\,max}$. To establish crack faces friction factor f_c at transverse shear fragments of fractured beam specimen containing crack faces were cut out and tested as a friction pair according to Amontons Coulomb's law using the original device and technique described in [36]. On the base of test results the fatigue crack growth rate curves in logarithmic coordinates ΔK vs. V were built by approximation of experimental data points with S-lines. These graphical dependencies for normal tension and transverse shear were used for determination of fatigue crack growth resistance characteristics, namely: basic – fatigue threshold ΔK_{th} and fracture toughness ΔK_{fc}, as the values of ΔK for crack growth rate $V = 10^{-10}$ and 10^{-4} m/cycle, respectively; auxiliary – $\Delta K_{1\text{-}2}$ and $\Delta K_{2\text{-}3}$, which indicates the beginning and the end of middle-amplitude region of curve; ΔK^* for crack growth rate $V = 10^{-7}$ m/cycle; parameters C and n of Paris's equation $V = C(\Delta K)^n$, which approximates the middle-amplitude region of curve.

Metallographic and fractographic analyses were performed on the scanning electronic microscope Zeiss EVO 40XVP. For fractographic analysis fragments of specimens containing crack faces were cut out.

3. Results and discussion

It is well known that during tempering of quenched carbon steel the diffusion process of martensite disintegration and carbide transformation occurs, resulting formation of ferrite-cementite microstructure of different dispersion and morphology. So, tempering at 650°C causes formation of high tempered martensite consisting of plate-globular cementite formations of irregular shape that fill ferritic matrix. It should be noted that cementite plates in structures after hardening and high tempering (Fig. 2) are similar in appearance to granular pearlite and is characterized by higher dispersion caused by increasing their sphericity, unlike oblong shape of cementite plates in cases when tempering is performed at lower temperatures [37].

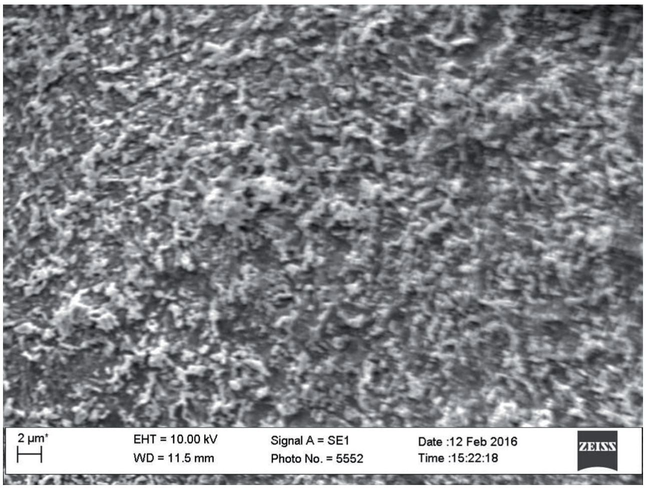

Fig. 2. Microstructure of high tempered 65G steel

Comparing the results of static tension tests of cylindrical specimens (Table 2) with those obtained previously for steel 65G tempered at 600°C [36] it can be seen that slight increase of temperature leads to some increase of characteristics of ductility. Strength characteristics in their turn slightly reduce.

Table 2.
Mechanical properties of investigated high tempered steel

Tempering temperature $t_α$, ºC	Yield stress $σ_y$, MPa	Ultimate stress $σ_u$, MPa	Elongation $δ_{10}$, %	Reduction of area ψ, %	Hardness HRC
650	830	950	16	52	30

The fatigue crack growth rate curves of investigated steel with high tempered martensite structure were built for crack growth rate in a range that covers up to 6 orders for normal tension (Fig. 3a) and transverse shear (Fig. 3b), taking into account experimentally determined crack faces friction factor $f_c = 0.43$. The curves describe the fatigue crack growth at low- (ΔK_I < 15 MPa√m, ΔK_{II} < 24 MPa√m), medium- (ΔK_I = 15-72 MPa√m, ΔK_{II} = 24-116 MPa√m) and of high-amplitude loading (ΔK_I > 72 MPa√m, ΔK_{II} > 116 MPa√m) for both modes of fracture. The medium-amplitude area for normal tension, as so as for transverse shear lies within the range of fatigue crack growth rate $V \approx 2 \cdot 10^{-8}$-$10^{-6}$ m/cycle.

a) b)

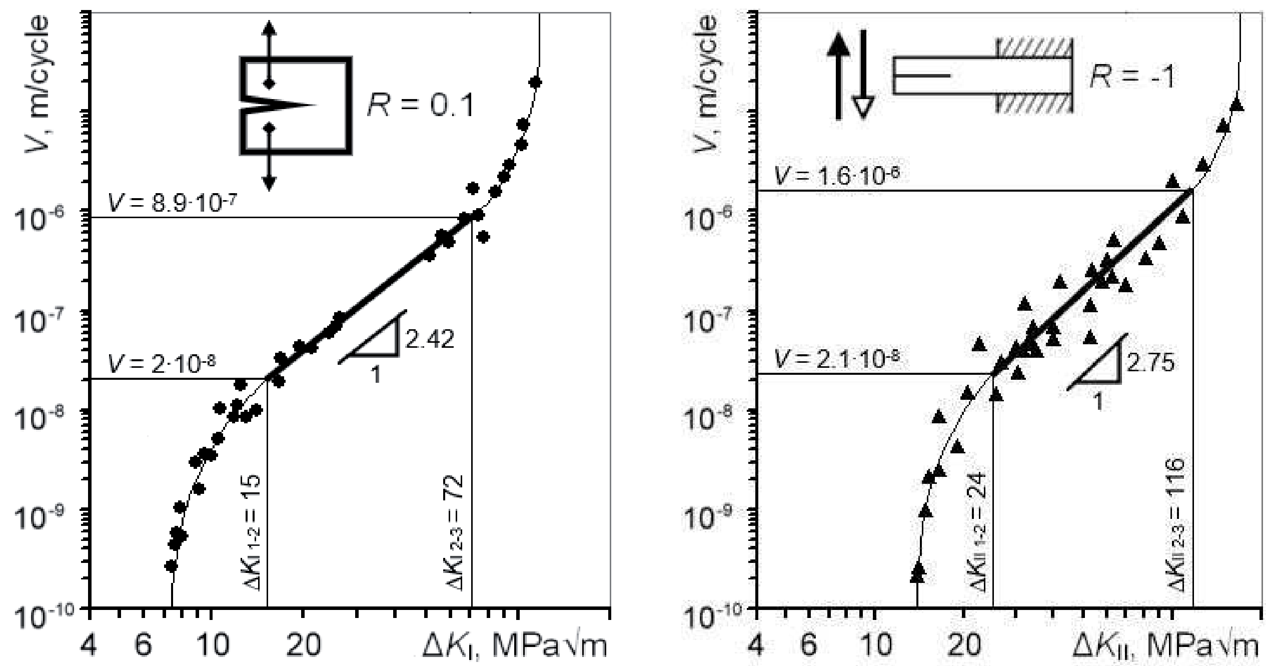

Fig. 3. Fatigue crack growth rate curves of high tempered 65G steel: a – normal tension; b – transverse shear ($f_c = 0.43$)

For transverse shear mode we can see the greater scatter of points on this region of curve (Fig. 3b). In contrast, the normal tension experimental points have much less scatter (Fig. 3a). This proofs that fatigue crack growth at transverse shear has intermittent nature that makes more complicated the process of approximation of experimental points. The fatigue crack growth resistance characteristics obtained from fatigue crack growth rate curves are represented in Table 3.

On the base of fractographic analysis it was found that at normal tension grooves and pits forms on the crack surface, whereas the cleavage facets are practically absent (Figs. 4a,b). It is well correspond with the results obtained previously [38] for vanadium alloyed steel. In contrast, at transverse shear smooth delamination regions and cut tongues appears (Figs. 4c,d). It should be noted that at relatively low fatigue crack growth rate $V \approx 2 \cdot 10^{-8}$ m/cycle (Fig. 4c) the cut tongues appears quite often, while at high

Table 3.
Fatigue crack growth resistance characteristics of investigated high tempered steel

Fracture mode	Main characteristics		Auxiliary characteristics			Paris's equation parameters	
	ΔK_{th}	ΔK_{fc}	ΔK_{1-2}	ΔK_{2-3}	ΔK^*	C	n
	MPa√m					$(MPa\sqrt{m})^{-n}$×m/cycle	
Mode I	7.4	118	15	72	30	$2.853 \cdot 10^{-11}$	2.42
Mode II	13.8	170	24	116	43	$3.359 \cdot 10^{-12}$	2.75

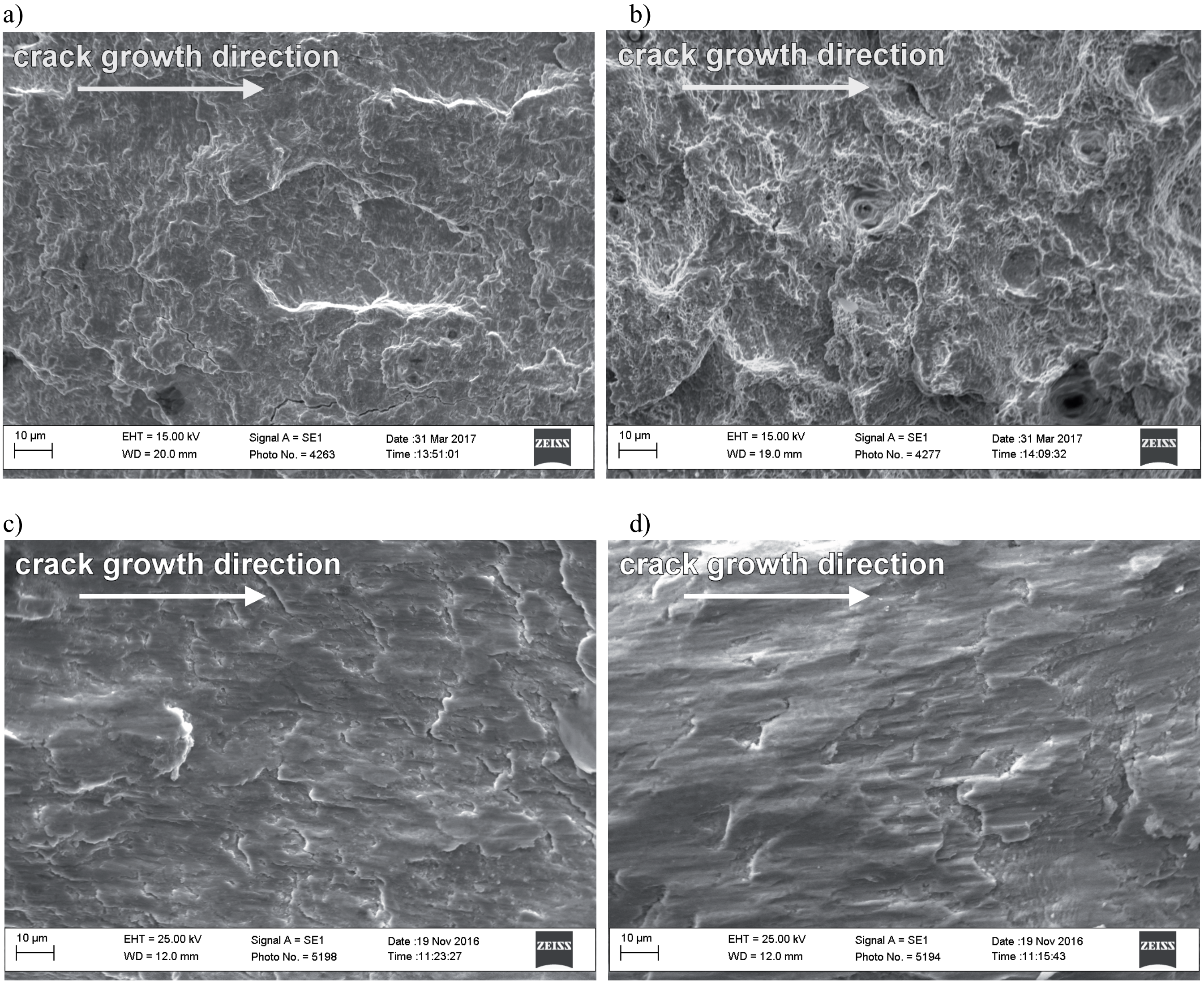

Fig. 4. Microfractograms of investigated high tempered steel for normal tension (a, b) and transverse shear (c, d): a), c) $V \approx 2 \cdot 10^{-8}$ m/cycle, b), d) $V \approx 10^{-6}$ m/cycle

speeds $V \approx 10^{-6}$ m/cycle the smooth delamination regions dominates (Fig. 4d).

Comparison of the crack faces friction factor $f_c = 0.43$ of steel with structure with values established earlier [36] for finer high tempered martensite and low tempered martensite structure is represented on Figure 5. As can be seen, there is a clearly visible tendency of crack faces friction factor reducing due to reduction of the yield stress of steel.

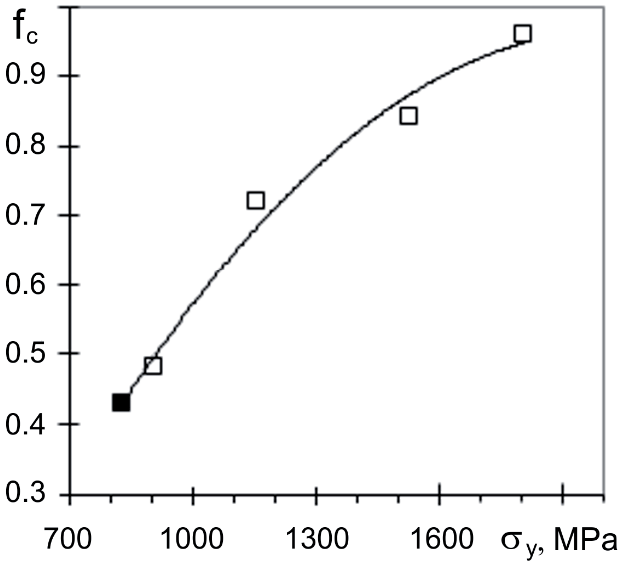

Fig. 5. Dependence of crack faces friction factor on yield stress of investigated tempered steel. The white markers correspond to the results, obtained earlier [36]

The explanation for this is that the crack faces friction factor is highly affected by fracture surface relief features formed on both cracks faces at transverse shear fatigue fracture. Moreover, the most important are geometrical parameters of microroughnesses, which in their turn are affected by the phase composition and microstructure of steel, that is by the form of cementite formations and by distance between carbide particles.

4. Conclusions

The main $\Delta K_{I\,th} = 7.4$ MPa√m, $\Delta K_{II\,th} = 13.8$ MPa√m, $\Delta K_{I\,fc} = 118$ MPa√m, $\Delta K_{II\,fc} = 170$ MPa√m and auxiliary fatigue crack growth resistance characteristics and parameters of Paris's equations at normal tension and transverse shear are determined. These characteristics can be used for workability assessment of high tempered 65G steel at rolling contact fatigue conditions.

References

[1] U.P. Singh, R. Singh, Wear investigation of wheel and rail steels under conditions of sliding and rolling-sliding contact with particular regard to microstructural parameters, Wear 170/1 (1993) 93-99, doi: 10.1016/0043-1648(93)90355-P.

[2] W. Zhong, J.J. Hu, P. Shen, C.Y. Wang, Q.Y. Lius, Experimental investigation between rolling contact fatigue and wear of high-speed and heavy-haul railway and selection of rail material, Wear 271/9-10 (2011) 2485-2493, doi: 10.1016/j.wear.2010.12.053.

[3] J.H. Beynon, J.E. Garnham, K.J. Sawley, Rolling contact fatigue of three pearlitic rail steels, Wear 192 (1996) 94-111, doi: 10.1016/0043-1648(95)06776-0.

[4] Y. Miyashita, Y. Yoshimura, J. Xu, M. Horikoshi, Y. Mutoh, Subsurface crack propagation in rolling contact fatigue of sintered alloy, International Journal Series A Solid Mechanics and Material Engineering 46/3 (2003) 341-347.

[5] E. Bormetti, G. Donzella, A. Mazzu, Surface and subsurface cracks in rolling contact fatigue of hardened components, Tribology Transactions 45/3 (2002) 274-283.

[6] A. Mazzu, L. Solazzi, M. Lancini, C. Petrogalli, A. Ghidini, M. Faccoli, An experimental procedure for surface damage assessment in railway wheel and rail steels, Wear 342-343 (2015) 22-32.

[7] G. Donzella, A. Mazzu, C. Petrogalli, Experimental and numerical investigation on shear propagation of subsurface cracks under rolling contact fatigue, Procedia Engineering 109 (2015) 181-188, doi: 10.1016/j.proeng.2015.06.230.

[8] P. Clayton, X. Su, Surface initiated fatigue of pearlitic and bainitic steels under water lubricated rolling/sliding contact, Wear 200/1-2 (1996) 63-73, doi: 10.1016/S0043-1648(96)07250-X.

[9] W.R. Tyfour, J.H. Beynon, A. Kapoor, Deterioration of rolling contact fatigue life of pearlitic rail steel due to dry-wet rolling-sliding line contact, Wear 197/1-2 (1996) 255-265.

[10] K. Cvetkovski, J. Ahlstrom, M. Norell, C. Persson. Analysis of wear debris in rolling contact fatigue cracks of pearlitic railway wheels, Wear 314/1-2 (2014) 51-56, doi: 10.1016/j.wear.2013.11.049.

[11] H. Matsunaga, H. Komata, J. Yamabe, Y. Fukushima, S. Matsuoka, Effect of size and depth of small defect on the rolling contact fatigue strength of bearing steel JIS-SUJ2, Procedia Materials Science 3 (2014) 1663-1668, doi: 10.1016/j.mspro.2014.06.268.

[12] M. Guagliano, L. Vergani, Prediction of the propagation of an internal crack under rolling contact loads by a weight function approach, Key Engineering Materials 251-252 (2003) 473-484.

[13] S. Deng, L. Hua, X. Han, S. Huang, Investigation of rolling contact fatigue cracks in ball bearings, International Journal of Fracture 188/1 (2014) 71-78.

[14] Y. Liu, B. Stratman, S. Mahadevan, Fatigue crack initiation life prediction of railroad wheels, International Journal of Fatigue 28/7 (2006) 747-756.

[15] P.L. Ko, S.S. Iyer, H. Vaughan, M. Gadala, Finite element modelling of crack growth and wear particle formation in sliding contact, Wear 251/1-12 (2001) 1265-1278.

[16] V.T. Troshchenko, G.V. Tsybanev, A.O. Khotsyanovsky, Two-parameter model of fretting fatigue crack growth, Fatigue & Fracture of Engineering Materials & Structures 17/1 (1994) 15-23, doi: 10.1111/j.1460-2695.1994.tb00769.x.

[17] A. Mazzu, A numerical approach to subsurface crack propagation assessment in rolling contact, Fatigue & Fracture of Engineering Materials & Structures 36/6 (2013) 548-564.

[18] K. Aslantas, S. Tasgetiren, Edge spalling formation in a plate due to moving compressive load, Turkish Journal of Engineering & Environmental Sciences 27/5 (2003) 333-338.

[19] R. Lunden, Elastoplastic modelling of subsurface crack growth in rail/wheel contact problems, Fatigue & Fracture of Engineering Materials & Structures 30/10 (2007) 905-914.

[20] G. Donzella, M. Faccoli, A. Ghidini, A. Mazzu, R. Roberti, The competitive role of wear and RCF in a rail steel, Engineering Fracture Mechanics 72/2 (2005) 287-308.

[21] S. Bogdanski, M.W. Brown, Modelling the three-dimensional behaviour of shallow rolling contact fatigue cracks in rails, Wear 253/1-2 (2002) 17-25, doi: 10.1016/S0043-1648(02)00078-9.

[22] O.P. Datsyshyn, V.V. Panasyuk, A.Y. Glazov, Modeling of fatigue contact damages formation in rolling bodies and assessment of their lifetime, Wear 271/1-2 (2011) 186-194, doi: 10.1016/j.wear.2010.10.023.

[23] X. Xu, D. Cho, Y. Chang, J. Choi, Y. Kim, H. Jun, J. Seo, D. Kim, Evaluation of slant crack propagation under RCF in railway rail, Journal of Mechanical Science and Technology 25/5 (2011) 1215-1220.

[24] J. Seo, S. Kwon, H. Jun, D. Lee, Fatigue crack growth behavior of surface crack in rails, Procedia Engineering 2 (2010) 865-872.

[25] T.M. Lenkovs'kyi, Determination of the characteristics of cyclic crack resistance of steels under transverse shear (a survey), Materials Science 50/3 (2014) 340-349.

[26] Y.L. Ivanyts'kyi, T.M. Lenkovs'kyi, I.A. Verhun, S.T. Shtayura, Investigation of the kinetics of fatigue macrocracks under transverse shear, Materials Science 52/3 (2016) 349-356.

[27] G.V. Tsybanev, P.Y. Kravets, A.O. Khotsyanovskii, A method of testing for crack resistance under a cyclic shearing load, Strength of Materials 24/1 (1992) 97-103, doi: 10.1007/BF00777234.

[28] H. Matsunaga, N. Shomura, S. Muramato, M. Endo, Shear mode threshold for a small fatigue crack in a bearing steel, Fatigue & Fracture of Engineering Materials & Structures 34/1 (2011) 72-82.

[29] V. Doquet, Q.H. Bui, G. Bertolino, E. Merhy, L. Alves, 3D shear-mode fatigue crack growth in maraging steel and Ti-6Al-4V, International Journal of Fracture 165/1 (2010) 61-76.

[30] H. Nishizawa, T. Ogawa, A mode II fatigue crack growth characteristics and experimental evaluation of the crack driving force, Journal of the Society of Materials Science 54/12 (2005) 1295-1300.

[31] S. Okazaki, K. Wada, H. Matsunaga, M. Endo, The influence of static crack-opening stress on the threshold level for shear-mode fatigue crack growth in bearing steels, Engineering Fracture Mechanics 174 (2017) 127-138.

[32] State Standard GOST 1497-84 (1984) Metals. Methods of tension test, Moscow: Izd. Standartov, 36 p. (in Russian).

[33] Methodical guidelines RD 50-345-82 (1983) Methods for mechanical tests of metals, Determination of the characteristics of crack-growth resistance (fracture toughness) under cyclic loading, Moscow: Izd. Standartov, 95 p. (in Russian).

[34] Patent for a useful model no. 73715 (2012) Installation for the formation of a mode II fatigue crack in beam specimens, Kyiv: DP "Ukrpatent", 4 p. (in Ukrainian).

[35] State Standard DSTU 8601:2015 (2016) Calculation and strength tests, The method for determining crack

growth resistance characteristics under transverse shear of metals at room temperature, Kyiv: DP “UkrNDNC”, 27 p. (in Ukrainian).

[36] Y.L. Ivanytskyj, T.M. Lenkovskiy, Y.V. Molkov, V.V. Kulyk, Z.A. Duriagina, Influence of 65G steel microstructure on crack faces friction factor under mode II fatigue fracture, Archives of Materials Science and Engineering 82/2 (2016) 49-56.

[37] Y. Yamada, Materials for Springs, Springer Science & Business Media, 2007, 377 p., ISBN 978-3-540-73812-1.

[38] O.P. Ostash, I.M. Andreiko, V.V. Kulyk, O.I. Babachenko, V.V. Vira, Influence of the mode of thermal treatment and load ratio on the cyclic crack-growth resistance of wheel steels, Materials Science 45/2 (2009) 211-219, doi.org/10.1007/s11003-009-9112-8.